2024-01-2166 Published 09 Apr 2024



# Electric Vehicle Modeling: Advanced Torque Split Analysis across Different Architectures

David Oswald, Jacqueline Escobar, Guoyuan Wu, Heejung Jung, and Matthew Barth

University Of California Riverside

Citation: Oswald, D., Escobar, J., Wu, G., Jung, H. et al., "Electric Vehicle Modeling: Advanced Torque Split Analysis across Different Architectures," SAE Technical Paper 2024-01-2166, 2024, doi:10.4271/2024-01-2166.

Received: 23 Nov 2023

Revised: 20 Jan 2024

Accepted: 21 Jan 2024

### **Abstract**

he proliferation of electric vehicles (EVs) is resulting in a big transition in the automotive industry, with the goal of reducing greenhouse gas emissions and improving energy efficiency. There are a variety of different architectural configurations and power distribution strategies that can be optimized for drivability performance, all-electric range, and overall efficiency. This paper describes the efforts of the research team in exploring different EV architectures to better understand their impacts on system performance in terms of energy efficiency and vehicle drivability. In search for an ideal powertrain architecture for a shared-use EV, the research team conducted a comprehensive analysis of a various EV architectures (including RWD and AWD) with different motor parameters, considering a spectrum of targeted vehicle technology specifications such as acceleration and braking performance, and fuel economy. To quantify these performance indices, a model-based design approach

was utilized, leveraging the EV development tools developed by MATLAB/Simulink and Simscape. Standard driving cycles, e.g., Highway Fuel Economy Driving Schedule (HWFET) and Urban Dynamometer Driving Schedule (UDDS) were utilized to evaluate different EV powertrain architectures and rear/front wheel power splits. The simulation results showed that for the architectures (with respective parameters) investigated in this study, the AWD architectures have higher energy efficiency than the RWD architecture in the range of 5.4 – 37.9%. To further scrutinize performance across a wide spectrum of driving scenarios, we introduced a specialized modal driving profile. This comprehensive profile encompasses a diverse array of modal events, including varying acceleration rates and steady-state speeds, among others. In our analysis, we found that a standard torque split of 50/50 keeps a good balance between energy efficiency and drivability for our target AWD architecture.

## Introduction

hared mobility, represented by the rise of ridesharing platforms and car-sharing systems, is undergoing a major change towards sustainability, particularly by embracing vehicle electrification. In light of this transition, the research team is conducting a project reconceptualizing the Cadillac Lyriq [1], not just as a symbol of luxury and excellence, but as a leading figure in the shared, connected, automated, and electric vehicle domain. This project focuses on enhancing the driving range, which is essential for shared mobility use. The motivation behind this transformation is largely driven by regulations, especially California's Senate Bill SB-1014, the Clean Miles Standard [2], which mandates electrification of all shared mobility vehicles in the state.

The project goal is to redesign a Cadillac Lyriq, so that it becomes an attractive option for many shared-vehicle use cases. For example, with extended range, the vehicle could be an excellent option for transportation network companies like Uber and Lyft, that want to offer

a larger, luxury vehicle in their fleets. As another option, our vehicle design could play a significant role in innovative carsharing systems that serve disadvantaged communities, where driving range may be one consideration. Moreover, its adaptability can address gaps in traditional public transit systems by offering solutions to multiple passengers, and can also meet the demands of individual users who prioritize range. In the EV landscape, the Cadillac Lyriq keeps a good balance in terms of range, price, acceleration, and economy from other brands as shown in Figure 1–3.

Thus, a strategic pathway to achieving an enhanced driving range could potentially involve the following approach:

 Choosing an architecture (e.g., AWD or RWD) and a motor configuration that find a balance between energy efficiency and driving performance under financial constraints. In general, almost all EVs typically have better MPGe for RWD compared to its AWD versions. AWD systems usually add more

#### **FIGURE 1** Market survey on fuel economy vs. acceleration.

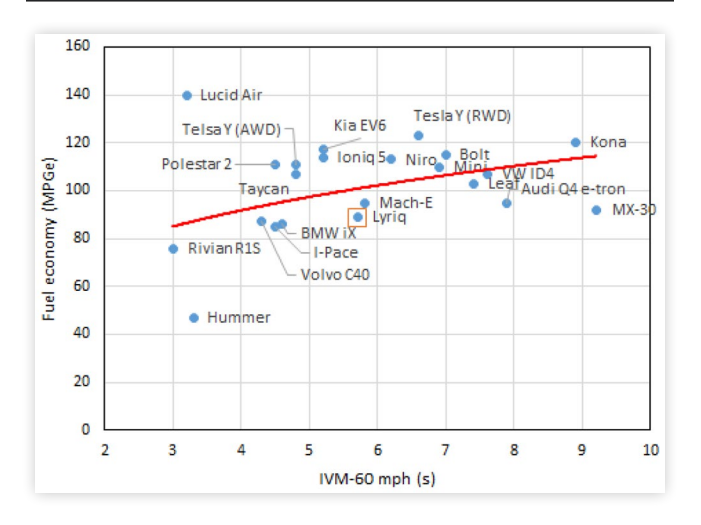


#### FIGURE 2 Market survey on price vs. range.

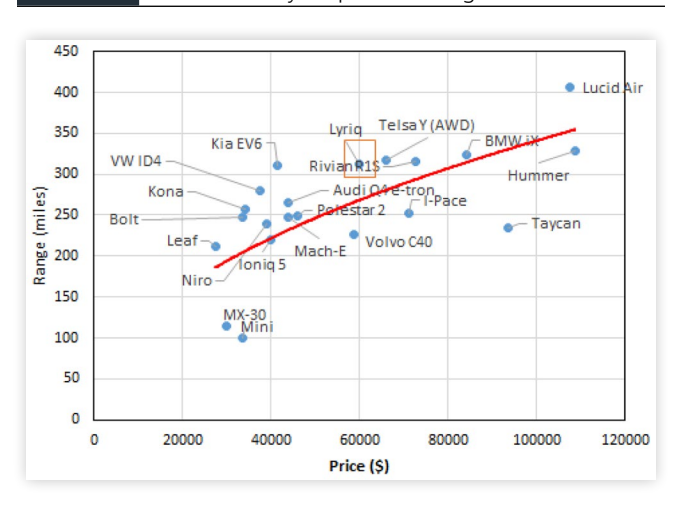
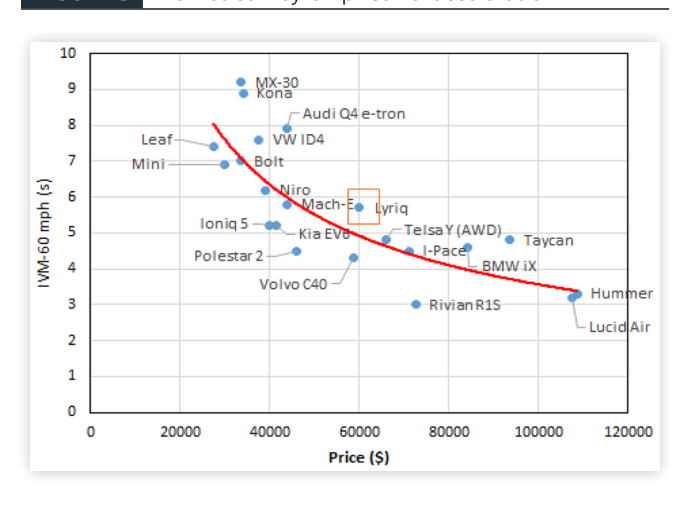


#### FIGURE 3 Market survey on price vs. acceleration.



- weight and less efficiency with their complex drivetrains. However, for the Lyriq, it has been noted in the literature that the AWD version does provide a slight increase in MPGe [3];
- Adjusting the motor control, with particular emphasis on dynamic torque vectoring, especially in possible configurations housing multiple motors, to enhance both economy and range;
- Employing an eco-friendly predictive speed trajectory algorithm for connected and automated electric vehicles developed by the research team [4]; and
- Implementing innovative techniques focusing on reducing vehicle weight and minimizing aerodynamic drag.

In this paper, we will focus on the architecture evaluation and torque split analysis that may provide further insight into EV performance in terms of both energy efficiency and driving performance. The rest of this paper is organized as follows. First, prior research efforts related to torque split are presented in the *Literature Review* section. Then, the dataset and methodology used in our study are described in the *Methodology* section. Next, the results and their discussion are described in the *Results* and *Discussion* sections. Finally, conclusions and future work are presented in the *Conclusions* section.

### Literature Review

Torque split analyses have been developed over the years, for all types of vehicle drivetrains. In [5], torque split predictions between front and rear axles in all-wheel-drive (AWD) vehicles are presented. The proposed model considers factors like dynamic weight transfer, tire stiffness, and shaft stiffness to gain a better understanding of how these factors affect torque distribution. The authors also analyzed three AWD subsystems to comprehend the torque split mechanism and achieved a reasonable correlation with test data. The results suggested that the simplified model should be used to predict torque on driveline components with improved accuracy.

In [6], a torque distribution control strategy for a hybrid electric vehicle powertrain was proposed. The authors used MATLAB, Cruise, and Simulink to construct powertrain models and analyze vehicle performance under the new European driving cycle (NEDC) conditions. The simulation results demonstrated that the torque distribution control strategy effectively managed the vehicle's output torque and promptly responded to varying vehicle operating conditions, emphasizing the significance of torque distribution. Using MATLAB and Simulink, the authors in [7] modeled and compared torque distributions between the front and rear drives in an AWD electric vehicle. Their proposed torque-splitting method is based on weight distribution, acceleration

conditions, and road gradient angles, resulting in an improvement in the vehicle's stability and performance. In [8], a Non-dominated Sorting Genetic Algorithm (NSGA-II) was proposed in MATLAB/Simulink to determine the optimal torque-split ratio for a dual-motor electric vehicle, giving equal importance to both dynamic and efficiency performance of the vehicle. The results demonstrated that optimizing the torque split ratio could enhance the vehicle's efficiency by enabling the motors to operate in a more efficient range for the same drive cycle demands while maintaining the required dynamic performance.

The authors in [9] proposed a MATLAB/Simulink control method that relies on a finite-set model-based predictive control (FS-MBPC) algorithm to regulate the torque of both motors and the flux level within the machine. Similarly, a control algorithm was also proposed in [10], where the authors conducted an experiment using two motors to verify the algorithm performance. The results showed that both motors operated on the optimal operation line while adhering to the desired battery power limitation within the optimum range. In [11], a dynamic programming algorithm was developed for torque distribution in four in-wheel motor drive electric vehicles to optimize energy efficiency. The algorithm was verified through simulation and experiment under various driving cycles and the torque distribution control models were built in the MATLAB/Simulink software. The results showed that the proposed torque distribution strategy effectively improved energy efficiency and control stability in AWD electric vehicles. A slip-ratio-based torque distribution control strategy for electric vehicles was presented in [12] to maintain stability and avoid slippage in split friction regions. The strategy, involving upper, middle, and lower controllers, distributed driving force to the four wheels while ensuring a guaranteed yaw moment. It outperformed fixed torque distribution methods in simulation experiments using CarSim and MATLAB/Simulink.

## Methodology

In this study, we consider three major architectures as described below.

## **Architecture Definition and Power Flow**

As shown in Figure 4, Architecture 1 is a rear-wheel-drive (RWD) configuration that uses a single 225kW motor. Architecture 2 is an AWD configuration using two 169kW motors, one in front and the other in rear (see Figure 5). Finally, Figure 6 shows Architecture 3 which is another AWD configuration. However, it uses different sized motors for the front (150 kW) and rear (180 kW). The power flow of each architecture (during propulsion) is also depicted as arrows in the respective figure.

**FIGURE 4** Architecture 1 is an RWD configuration that uses a single 225kW motor.

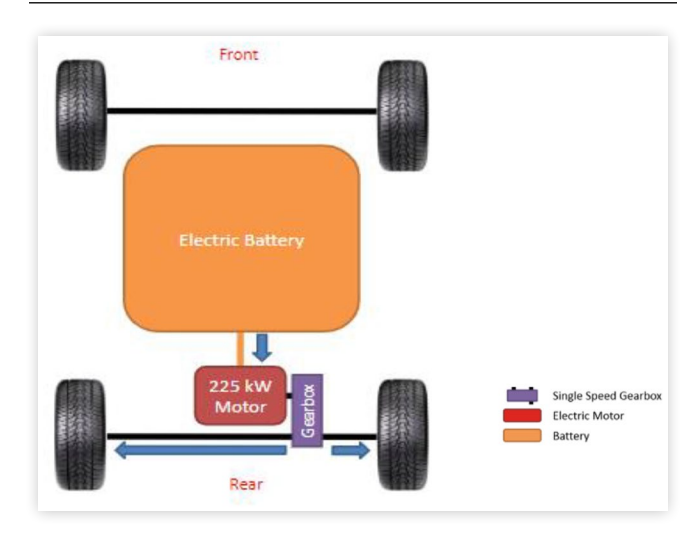
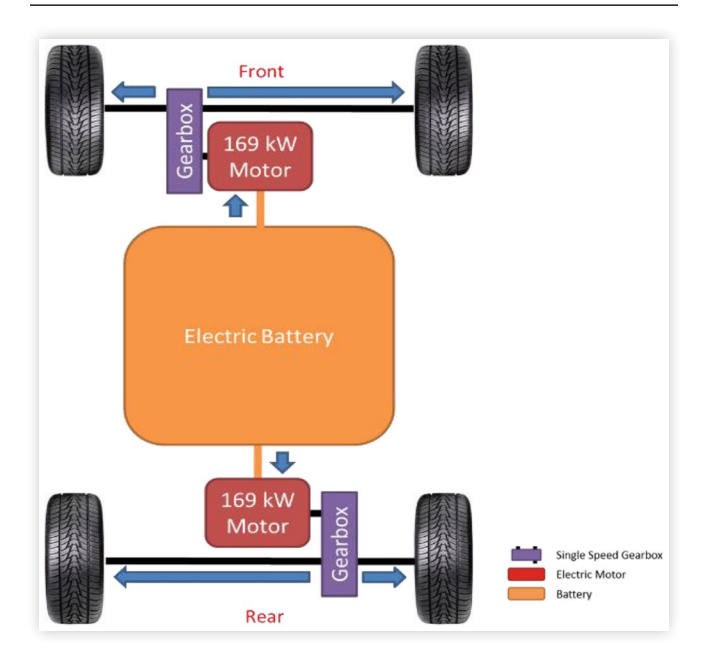


**FIGURE 5** Architecture 2 is an AWD configuration using two 169kW motors, one in front and the other in rear.



## **Torque Split Decoupling**

To evaluate the system performance across different architectures, the first step in our methodology involved calibrating both RWD electric vehicle (EV) model and AWD EV model in MATLAB/Simulink, as shown in Figure 7. It is also noted that the AWD EV model initially utilized a Hamiltonian method [14] for torque split optimization where the torques of the front and rear motors were highly coupled.

To enable more flexible analysis of torque split between front and real motors in this study, we identified the key MATLAB/Simulink blocks and model parameters responsible for torque distribution between the front and rear electric motors, and then decoupled the control logic. Based on the investigation, the original MATLAB/Simulink

#### ELECTRIC VEHICLE MODELING: ADVANCED TORQUE SPLIT ANALYSIS ACROSS DIFFERENT ARCHITECTURES

**FIGURE 6** Architecture 3 is another AWD configuration where the power of the front motor is 150 kW and the rear one is 180 kW.

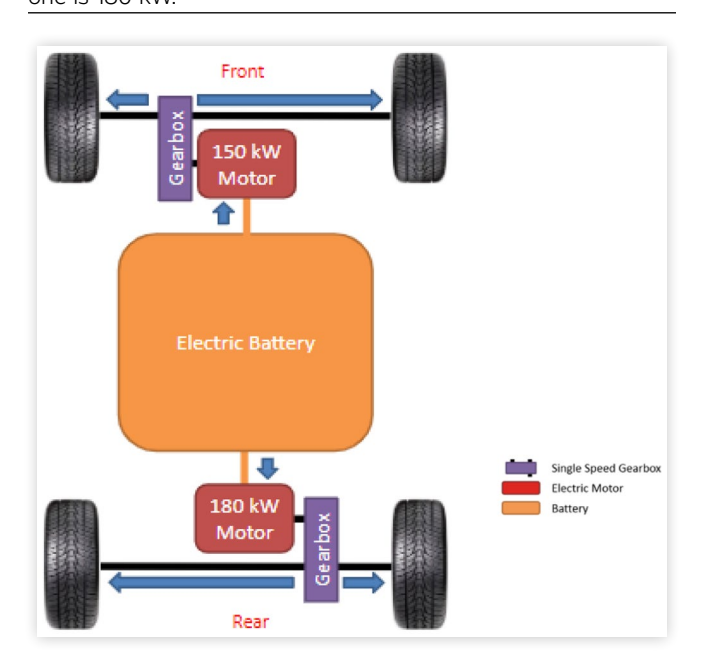
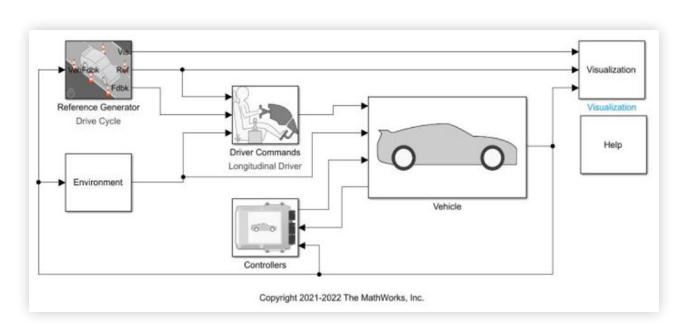


FIGURE 7 EV reference model in Matlab/Simulink [13].

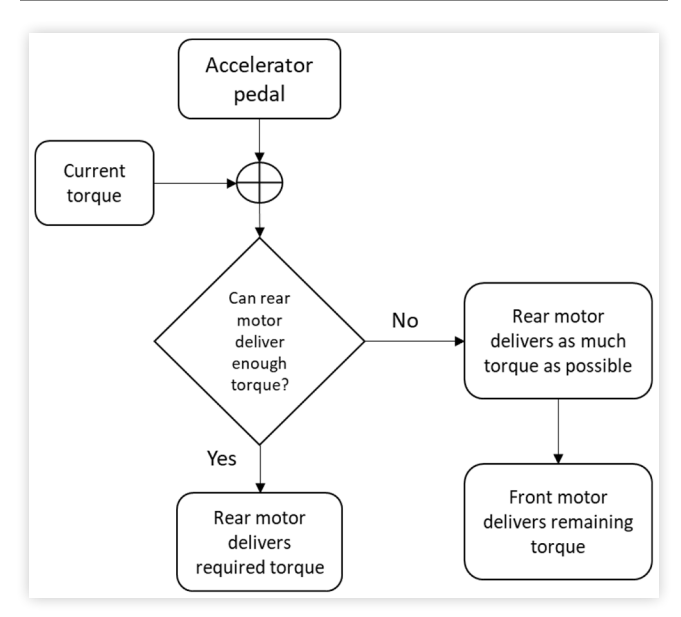


AWD EV model implemented a simplified Hamiltonian method, as illustrated in the flowchart in Figure 8.

- Get current wheel torque demand: The method begins by obtaining the current wheel torque values for both the front and rear wheels.
- Get wheel torque command from accelerator pedal: It retrieves the wheel torque commands generated from the accelerator pedal position.
- 3. **Check if the rear motor can deliver enough torque:** The method checks whether the rear motor alone can deliver enough torque to meet wheel torque demand specified by the command from steps 1 and 2.
- 4. **Allocate torque to the front motor:** In cases where the rear motor cannot deliver the required torque, it gives the front motor a command to deliver the remaining torque.

The existing simplified Hamiltonian-based torque split method does not allow for free selection of torque split between the front and rear motors. To address this issue,

FIGURE 8 Flowchart of Hamiltonian method for torque split.

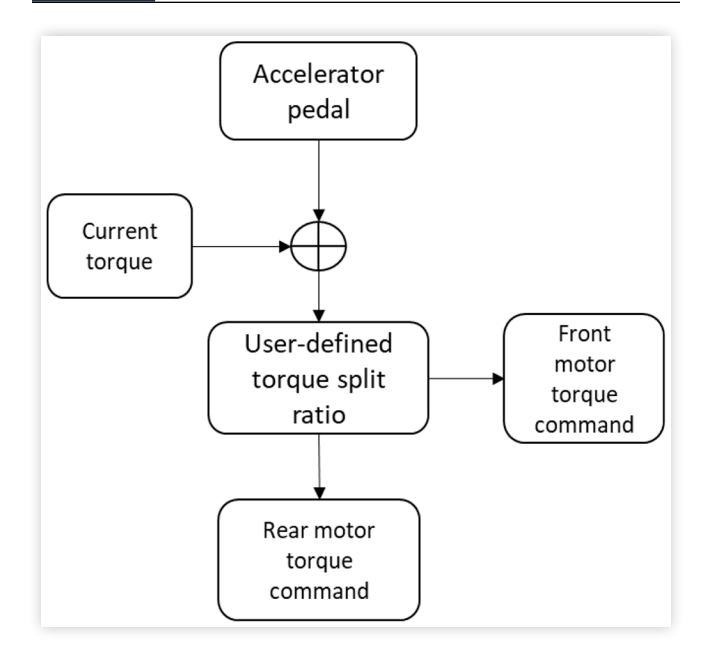


we performed a decoupling strategy to the original EV model by taking the following steps.

Firstly, we developed custom control logic within the MATLAB/Simulink model to enable decoupling of torque split for AWD. The logic also incorporated user-defined input parameters, allowing us to specify the desired torque split ratio for each motor. Figure 9 depicts the flowchart of the custom control logic:

- Get current wheel torque demand: The method begins by obtaining the current wheel torque values for both the front and rear wheels.
- 2. **Get wheel torque command from accelerator pedal:** It retrieves the wheel torque command generated from the accelerator pedal position.

**FIGURE 9** Flowchart of custom method for torque split.



 Gives command to front and rear motors to deliver torque based on user-defined ratio: In contrast to the Hamiltonian method, this approach commands the front and rear motors to deliver torque based on a user-defined ratio, allowing for manual control over the distribution of torque.

Secondly, to ensure that both the front and rear motors receive torque, we modified the torque command signals sent to each motor. We added these torque command signals together and applied the user-defined torque split ratio to determine the torque allocation for each motor.

Lastly, we conducted extensive testing and validation of the manual torque split implementation. This involved simulating a range of torque split ratios, including 90/10, 80/20, 70/30, 60/40, 50/50, 40/60, 30/70, 20/80, and 10/90 (rear motor/front motor), on two standard drive cycles: 1) HWFET [15] (a highway-based drive cycle); and 2) UDDS [15] (a city-based drive cycle). It is noted that while dynamic torque distribution is the norm in production AWD systems, the evaluation of constant torque splits in controlled testing environments complements real-world observations. It helps us gain a deeper understanding of the core characteristics and behaviors of different torque splits and provides essential data for optimizing AWD systems to excel in diverse driving situations. In addition, we evaluated the system performance across a wide spectrum of driving scenarios by introducing a specialized modal driving profile. This custom profile encompasses a diverse array of modal events, including varying acceleration rates and steadystate speeds.

## **Results**

## Comparison of Energy Economy across Different Architectures

To understand the performance of different architectures, energy economy (in MPGe) is evaluated using the aforementioned Matlab/Simulink model for each architecture under two standard drive cycles, i.e., HWFET and UDDS and the results are summarized in Table 1. Compared to both AWD architectures (i.e., Architecture 2 and Architecture 3), the RWD architecture is less energy efficient (ranging from 5.4% to 37.9%). In particular, RWD performs much worse than AWD in this study for City MPGe. A hypothesis is that the RWD motor is much larger in size and operating in a region with much less efficiency during city driving. In addition, Architecture 3 performs better than Architecture 2 under both highway and urban driving cycles, improving energy economy by 3.1% and 1.4%, respectively. It is noted that the torque split strategy applied to Architecture 2 and Architecture 3 in Table 1 is Hamiltonian method.

**TABLE 1** Energy economy (in MPGe) of different architectures across different driving cycles.

Drive Cycles	Architecture 1 (RWD)	Architecture 2 (AWD)	Architecture 3 (AWD)
HWFET	102.3	104.9 (2.5%)	108.1 (5.7%)
UDDS	89.1	113.8 (27.7%)	115.4 (29.5%)

<sup>\*</sup> Values in parentheses represent relative improvement compared to the RWD architecture.

### **Torque Split Analysis**

With the custom torque split control system in place, we proceeded to perform torque split analysis to evaluate the vehicle's performance under different torque distribution scenarios. We first defined a set of torque split scenarios, each representing specific driving conditions and objectives, which included the torque split ratios tested on the HWFET and UDDS drive cycles. Then, we evaluated the performance of the target electric vehicle for each torque split scenario based on predefined criteria, such as energy efficiency, acceleration time, and braking distance. This evaluation considers the outcomes of the extensive testing performed on the various drive cycles. To better understand the impacts of torque splits between rear and front motors, we performed a comprehensive analysis (under different torque splits) using Architecture 2 (where both motors have the identical power) in this study. Detailed results will be presented and discussed below.

<u>Table 2</u> presents the energy economy (in MPGe) using Architecture 2 for different torque splits under two drive cycles. As shown in the table, the energy economy does not vary significantly across different torque splits under HWFET (less than 1.0%) and UDDS drive cycles (less than 0.2%), respectively. However, the target EV (i.e., with Architecture 2) has much better energy economy for UDDS than HWFET (improved by up to 9.3%).

To evaluate the vehicle's drivability (e.g., acceleration and braking capabilities), <u>Table 3</u> summarizes the key performance metrics under different split ratios. These metrics include: 1) the time (in second) interval when accelerating (with wide open throttle) from initial vehicle movement (IVM) to 60 mph; 2) the time (in second) interval when accelerating from 50 mph to 70 mph; and 3)

**TABLE 2** Energy economy results (in MPGe) for Architecture 2 considering different split ratios at various driving cycles.

Rear/Front	HWFET	UDDS
90/10	104.1	113.8
80/20	104.6	113.8
70/30	104.8	113.8
60/40	104.9	113.8
50/50	104.9	113.8
40/60	105.1	113.8
30/70	105.1	113.9
20/80	104.9	114.0
10/90	104.5	113.9

#### ELECTRIC VEHICLE MODELING: ADVANCED TORQUE SPLIT ANALYSIS ACROSS DIFFERENT ARCHITECTURES

the braking distance (in meter) where decelerating from 60 mph to full stop. It can be observed from the table that the various torque splits exhibited substantial disparities in both acceleration and deceleration. Among these, the 50/50 torque split stands out as the configuration with the swiftest acceleration and the second shortest stopping distance. Specifically, the IVM-60mph acceleration time is 5 seconds (38.3% shorter than the 90/10 or 10/90 torque split); the 50-70mph acceleration time is 3.1 seconds (43.6% shorter than the 10/90 torque split); and the braking distance from 60mph is 59.5 meters (33.5% shorter than the 90/10 torque split but 3.3% longer than the best scenario, i.e., the 60/40 torque split). Additionally, Table 3 highlights a clear trend: as either the front or rear motor takes on a greater proportion of the torque demand, both acceleration and deceleration tend to decrease. This indicates that either front or rear-biased cases may limit the other motor torque, which prevents maximum utilization of all the available torque.

To provide better visualization of motor operations under different torque splits, Figure 10 and Figure 11 illustrate operating points along with motor efficiency maps for 50/50 torque split and 10/90 (rear/front) torque split (as examples) for HWFET and UDDS drive cycles, respectively. It is noted that both front motor and rear motor would operate evenly for torque split 50/50. Therefore, only the plots of front motor are presented herein.

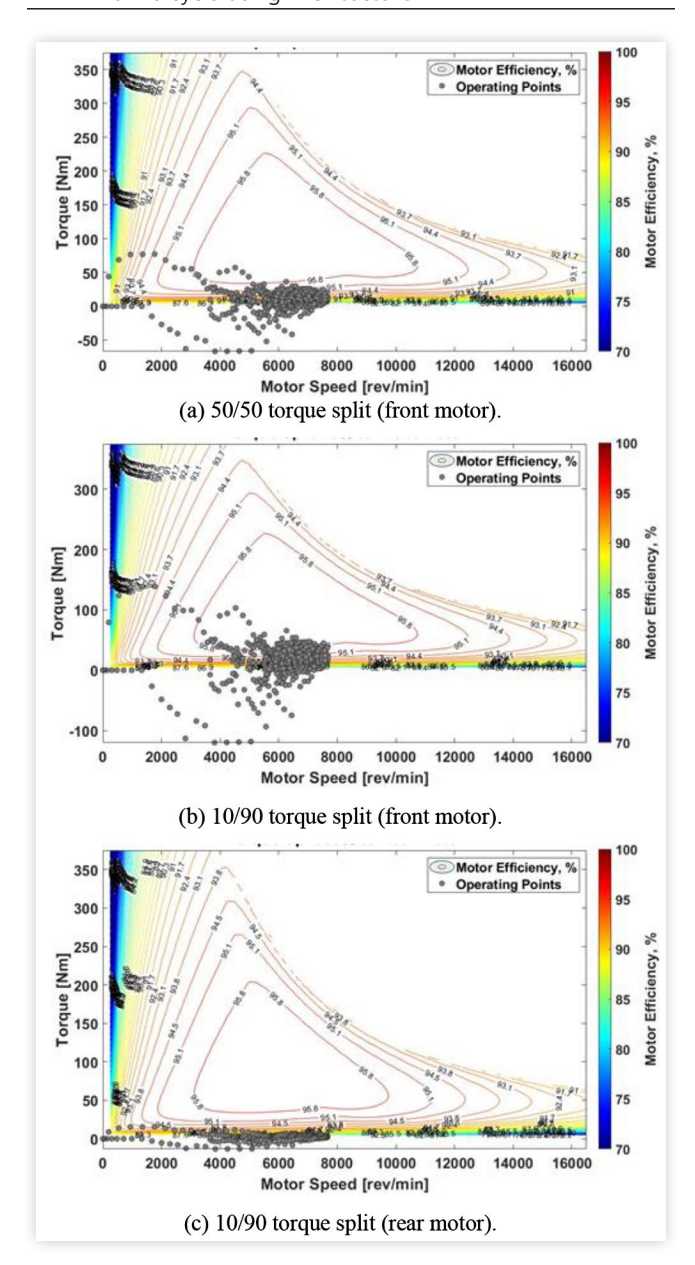
HWFET Drive Cycle As can be seen in Figure 10, except those startup or acceleration (from low speed) events, most of the operating points concentrate within the motor speed range between 5000 RPM and 8000 RPM. Compared to the torque split 50/50 scenario (see Figure 10 (a)), the operating points of front motor (i.e., Figure 10 (b)) in the torque split 10/90 (rear/front) scenario is more scattered as it needs to provide much more torque than the rear motor (i.e., Figure 10 (c)).

**UDDS Drive Cycle** Compared to HWFET drive cycle, most of the operating points in UDDS drive cycle fall in the lower motor speed range (below than 5000 RPM) due to lower vehicle speed in urban driving. In addition, there are more speed fluctuations (or stop-and-go maneuvers) in UDDS than HWFET. Obviously, due to the uneven

**TABLE 3** Other performance measures for Architecture 2 with different split ratios.

Rear/Front	IVM-60mph (sec)	50-70 mph (sec)	60-0 mph (meter)
90/10	8.1	5.3	89.5
80/20	6.9	4.7	67.6
70/30	6.1	4.1	61.1
60/40	5.5	3.8	57.6
50/50	5	3.1	59.5
40/60	5.4	3.7	61.0
30/70	6.0	4.3	67.3
20/80	7.1	5.0	69.5
10/90	8.1	5.5	75.8

**FIGURE 10** Motor contour plots (with operating points) for HWFET drive cycle using Architecture 2.

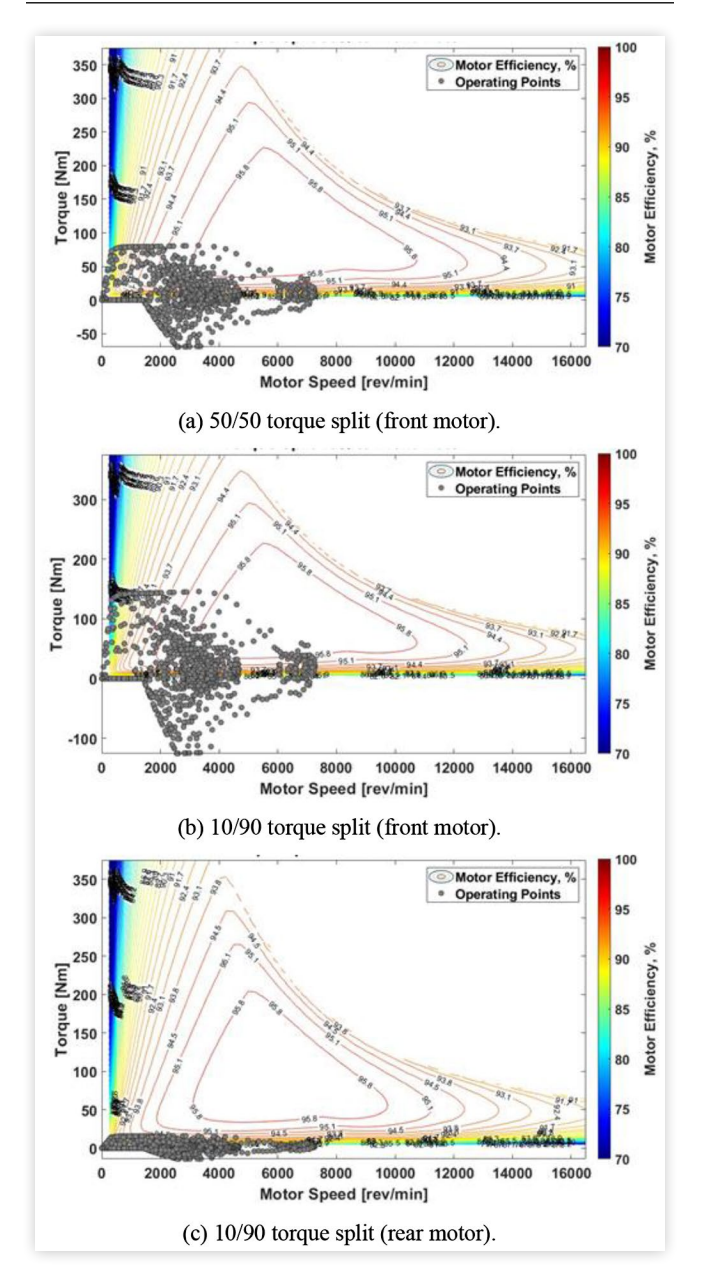


torque split, for the 10/90 torque split case, the operating points in the front motor (in <u>Figure 11(b)</u>) are much more scattered than the 50/50 torque split case (see <u>Figure 11(a)</u>), while the rear motor are much more concentrated (as shown in <u>Figure 11(c)</u>).

## Additional Tests across Different Modes

To better understand the system performance of Architecture 2 under different torque splits, we utilized a custom drive cycle, called MEC drive cycle [16] that focuses on specific modal events encompassing different levels of steady-state driving and different controlled acceleration rates. This cycle was originally developed for testing

**FIGURE 11** Motor contour plots (with operating points) for UDDS drive cycle using Architecture 2.



a vehicle across a wide range of its performance envelope, beyond what is seen in a typical vehicle activity-based driving cycle. The primary benefit of the MEC cycle lies in its ability to provide a clearer understanding of how each torque split performs in specific operational modes, as opposed to dealing with a complex dataset encompassing a representative driving cycle. As shown in <u>Figure 12</u>, the MEC cycle:

 covers most speed, acceleration, and specific power range modal events that span the entire performance envelope of most light-duty vehicles.

#### FIGURE 12 The MEC drive cycle [16].

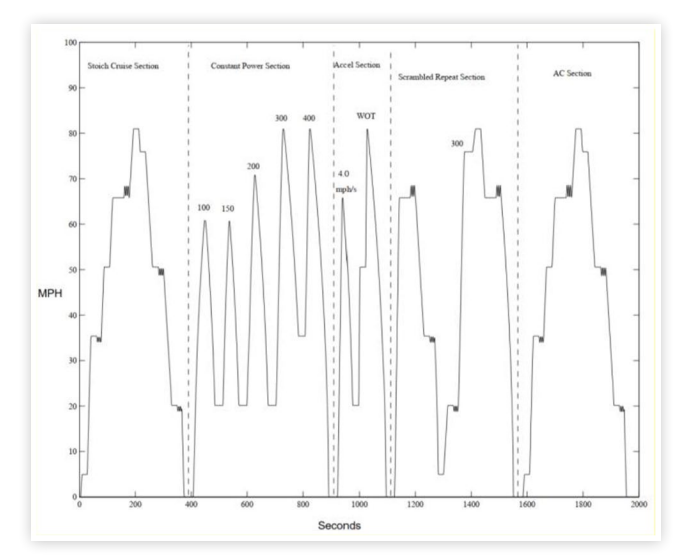
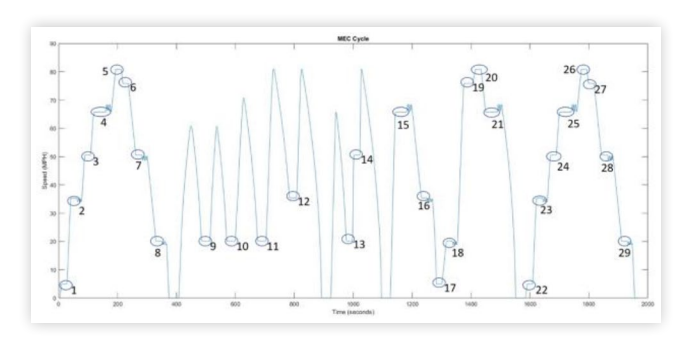


#### FIGURE 13 Steady states of MEC drive cycle [16].



- consists of various levels of accelerations; deceleration events; a set of constant cruise speeds (see those circles in <u>Figure 13</u>); speed-fluctuation driving; and constant power driving.
- consists of five different sections: steady-state cruise section, constant power section, constant acceleration section, scramble repeat section, and heavily loaded air conditioning hill section.

Using the MEC cycle, different torque splits were tested for the steady-state modes, and evaluated where the motor configurations could be improved (in terms of efficiency). This approach was particularly useful when choosing dynamic torque splitting.

<u>Tables 4</u> and  $\underline{5}$  show the efficiencies of front motor and rear motor, respectively, of Architecture 2 for each steady-state mode of the MEC profile circled in <u>Figure 13</u>, under each torque split ratio. As can be seen from both tables, the torque split of 50/50 keeps a good balance between both motors in terms of motor efficiency across various steady states. It also remains the most reliable split ratio during the simulation test (i.e., having the least total occurrences of "no available data point" when considering front and rear motors together).

**TABLE 4** Motor efficiency (front motor) for Architecture 2 considering different split ratios at MEC steady-state modes from figure 13.

Mode	50/50	10/90	20/80	30/70	40/60	60/40	70/30	80/20	90/10
1	92.4	89.4	90.0	92.4	92.5	92.0	91.1	88.8	N/A
2	87.6	92.3	91.6	90.3	88.9	87.1	94.2	92.3	86.7
3	90.0	93.8	93.4	92.6	91.5	87.7	85.5	91.9	85.6
4	91.7	94.5	94.0	93.5	92.8	90.1	86.8	83.2	83.6
5	93.1	95.2	94.9	94.5	94.0	92.0	89.5	84.7	83.3
6	92.4	94.9	94.5	94.0	93.3	90.9	88 4	83.7	N/A
7	89.6	93.6	93.2	92.3	91.2	87.2	84.9	N/A	N/A
8	N/A	89.1	88.3	87.6	N/A	N/A	N/A	N/A	N/A
9	N/A	89.1	88.4	87.6	N/A	N/A	N/A	N/A	N/A
10	N/A	89.1	88.4	87.6	N/A	N/A	N/A	N/A	N/A
11	N/A	89.1	88.4	87.6	N/A	N/A	N/A	N/A	N/A
12	87.1	91.9	91.1	89.8	88.5	85.9	N/A	N/A	N/A
13	N/A	89.1	88.3	87.6	N/A	N/A	N/A	N/A	N/A
14	90.3	93.9	93.5	92.7	91.8	88.1	86.0	92.8	94.8
15	91.7	94.5	94.0	93.4	92.7	90.0	86.6	83.0	N/A
16	87.1	92.1	91.3	89.9	88.5	85.9	N/A	N/A	N/A
17	N/A								
18	89.8	89.4	88.7	87.9	91.3	88.2	N/A	N/A	N/A
19	92.5	94.9	94.6	94.1	93.4	91.1	88.6	84.0	83.9
20	93.0	95.1	94.9	94.5	93.9	91.9	89.3	84.4	N/A
21	91.5	94.4	93.9	93.3	92.6	89.8	86.6	83.0	N/A
22	90.0	92.4	92.1	91.7	91.2	88.8	N/A	N/A	N/A
23	87.5	92.3	91.5	90.2	88.8	86.7	89.6	86.4	N/A
24	90.2	93.9	93.5	92.7	91.7	88.0	85.8	90.2	88.2
25	91.8	94.5	94.0	93.5	92.8	90.0	86.7	83.1	N/A
26	93.1	95.2	94.9	94.6	94.0	92.1	89.6	84.9	85.5
27	92.2	94.8	94.4	93.9	93.1	90.7	88.1	83.7	N/A
28	89.6	93.2	92.8	92.4	91.3	87.3	84.9	N/A	N/A
29	N/A	89.1	88.3	87.6	87.2	N/A	N/A	N/A	N/A

"N/A" means no data point available during the test.

# **Conclusions and Future Work**

In this study, we evaluate the impacts of different EV architectures, motor parameters and torque splits on energy efficiency and vehicle drivability, by leveraging the model-based design approach empowered by MATLAB/ Simulink and its EV development toolkit. We investigate both rear-wheel-drive (RWD) and all-wheel-drive (AWD), as well as a wide range of rear/front motor torque splits for AWD. Based on our modeling tools, we are seeing greater energy economy for the AWD (specific in this study), which matches the statement in [3]. The potential differences in masses and efficiencies for different-sized motors can contribute to the results. More specifically,

AWD architectures outperform the RWD architecture in the range from 5.4% to 37.9%. This is likely due to the more sophisticated torque split strategy. Furthermore, maintaining a torque split of 50/50 achieves a favorable equilibrium between energy efficiency and drivability performance for the specified AWD architecture.

As future work, we plan on improving our modeling tools and to dig deeper into this RWD/AWD issue. We will further investigate the impacts of architecture and torque splits in more comprehensive scenarios (e.g., presence of road grade). In addition, we will explore an online optimal torque split strategy for the target AWD EV architecture to improve energy efficiency without compromising vehicle drivability. The system performance will be evaluated using the model-in-the-loop testing approach enabled by Matlab/Simulink.

**TABLE 5** Motor efficiency (rear motor) for Architecture 2 considering different split ratios at MEC steady-state modes from figure 13.

Mode	50/50	10/90	20/80	30/70	40/60	60/40	70/30	80/20	90/10
1	92.4	N/A	88.8	91.1	92.0	92.5	92.4	90.0	89.4
2	87.6	86.7	92.3	94.2	87.1	88.9	90.3	91.6	92.3
3	90.0	85.6	91.9	85.5	87.7	91.5	92.6	93.4	93.8
4	91.7	83.6	83.2	86.8	90.1	92.8	93.5	94.1	94.6
5	93.2	84.0	85.3	89.9	92.2	94.0	94.5	94.8	95.0
6	92.9	N/A	84.3	88.9	91.5	93.7	94.4	94.7	95.0
7	89.6	N/A	N/A	84.9	87.2	91.2	92.3	93.2	93.6
8	N/A	N/A	N/A	N/A	N/A	N/A	87.6	88.3	89.1
9	N/A	N/A	N/A	N/A	N/A	N/A	87.6	88.4	89.1
10	N/A	N/A	N/A	N/A	N/A	N/A	87.6	88.4	89.1
11	N/A	N/A	N/A	N/A	N/A	N/A	87.6	88.4	89.1
12	87.1	N/A	N/A	N/A	85.9	88.5	89.8	91.1	91.9
13	N/A	N/A	N/A	N/A	N/A	N/A	87.6	88.3	89.1
14	90.3	94.8	92.8	86.0	88.1	91.8	92.7	93.5	93.8
15	91.7	N/A	83.0	86.6	90.0	92.7	93.4	94.0	94.5
16	87.1	N/A	N/A	N/A	85.9	88.5	89.9	91.3	92.1
17	N/A								
18	89.8	N/A	N/A	N/A	88.2	91.3	87.9	88.7	89.4
19	93.0	84.6	84.7	89.2	91.6	93.8	94.4	94.8	95.1
20	93.1	N/A	85.0	89.7	92.1	93.9	94.5	94.8	95.0
21	91.5	N/A	83.0	86.6	89.8	92.6	93.3	93.9	94.5
22	90.0	N/A	N/A	N/A	88.8	91.2	91.7	92.1	92.4
23	87.5	N/A	86.4	89.6	86.7	88.8	90.2	91.5	92.3
24	90.2	88.2	90.2	85.8	88.0	91.7	92.7	93.5	93.9
25	91.8	N/A	83.1	86.7	89.9	92.8	93.5	94.1	94.5
26	93.3	86.2	85.5	90.0	92.3	94.0	94.5	94.8	95.0
27	92.7	N/A	84.4	88.7	91.2	93.6	94.2	94.6	94.9
28	89.6	N/A	N/A	84.9	87.3	91.3	92.4	92.8	93.2
29	N/A	N/A	N/A	N/A	N/A	87.2	87.6	88.3	89.1

## References

- "The University of California at Riverside (UCR) EcoCAR Project," <a href="https://ecocar.engr.ucr.edu/">https://ecocar.engr.ucr.edu/</a>.
- 2. "SB-1014 California Clean Miles Standard and Incentive Program: Zero-Emission Vehicles," 2017-2018.
- 3. <a href="https://www.caranddriver.com/cadillac/lyriq-2023">https://www.caranddriver.com/cadillac/lyriq-2023</a>.
- 4. Jin, Q., Wu, G., Boriboonsomsin, K., and Barth, M., "Power-based Optimal Longitudinal Control for a Connected Eco-Driving System," *IEEE Transaction on ITS* 17, no. 10: 2900-2910.
- Sondkar, P., Gharpure, S., Schrand, V., and Attibele, P., "Longitudinal Vehicle Dynamics Modeling for AWD/4WD Vehicles to Study Torque Split between Front and Rear Axles," SAE Int. J. Adv. & Curr. Prac. in Mobility 2, no. 5 (2020): 2987-2996, doi:https://doi.org/10.4271/2020-01-1410.
- 6. Zhang, L., Dong, E., and Zhang, K., "Torque Distribution Control Strategy of Hybrid Electric Vehicle Powertrain,"

- in 2019 IEEE 3rd Information Technology, Networking, Electronic and Automation Control Conference (ITNEC), Chengdu, China, 2019, 1400-1403, doi:10.1109/ITNEC.2019.8729373.
- Agrawal, B., and Kirar, M.K., "Comparative Study for Torque Distribution between Front & Rear Drive in an All Wheel Drive Electric Vehicle," in 2023 IEEE Renewable Energy and Sustainable E-Mobility Conference (RESEM), Bhopal, India, 2023, 1-6, doi:10.1109/ RESEM57584.2023.10236042.
- 8. Castro, M.V. et al., "Non–Dominated Sorting Genetic Algorithm Based Determination of Optimal Torque–Split Ratio for a Dual–Motor Electric Vehicle," in *IECON 2021 47th Annual Conference of the IEEE Industrial Electronics Society*, Toronto, ON, Canada, 2021, 1-6, doi:10.1109/IECON48115.2021.9589555.
- 9. De Belie, F., De Brabandere, E., Druant, J., Sergeant, P. et al., "Model Based Predictive Torque Control of an Electric Variable Transmission for Hybrid Electric Vehicles," in 2016 International Symposium on Power Electronics, Electrical Drives, Automation and Motion

#### ELECTRIC VEHICLE MODELING: ADVANCED TORQUE SPLIT ANALYSIS ACROSS DIFFERENT ARCHITECTURES

- (SPEEDAM), Capri, Italy, 2016, 1203-1207, doi:10.1109/ SPEEDAM.2016.7525823.
- Kim, J. et al., "Control Algorithm for a Power Split Type Hybrid Electric Vehicle," in SPEEDAM 2010, Pisa, Italy, 2010, 1575-1580, doi:10.1109/SPEEDAM.2010.5542273.
- Adeleke, O., Li, Y., Chen, Q., Zhou, W. et al., "Torque Distribution Based on Dynamic Programming Algorithm for Four In-Wheel Motor Drive Electric Vehicle Considering Energy Efficiency Optimization," World Electric Vehicle Journal. 13, no. 10 (2022): 181, doi:https:// doi.org/10.3390/wevj13100181.
- 12. Ji, Y.-H., and Liu, Y.-C., "Slip-ratio-based Torque Distribution Control Strategy for Electric Vehicles Over Split Friction Regions," in 2017 IEEE Conference on Control Technology and Applications (CCTA), Maui, HI, 2017, 274-280, doi:10.1109/CCTA.2017.8062475.
- 13. Mathworks, "EV Reference Application," accessed December 2022, <a href="https://www.mathworks.com/help/autoblks/ug/electric-vehicle-reference-application.html">https://www.mathworks.com/help/autoblks/ug/electric-vehicle-reference-application.html</a>.
- 14. Njeh, M., Cauet, S., Coirault, P., and Martin, P., "H∞ Control Strategy of Motor Torque Ripple in Hybrid Electric Vehicles: An Experimental Study," *IET Control Theory and Applications* 5, no. 1 (2011): 131-144.
- 15. "40 CFR 600, Subpart B," <a href="https://www.ecfr.gov/current/title-40/chapter-l/subchapter-Q/part-600/subpart-B">https://www.ecfr.gov/current/title-40/chapter-l/subchapter-Q/part-600/subpart-B</a>.

16. Barth, M., An, F., Norbeck, J., and Ross, M., "Modal Emissions Modeling: A Physical Approach," *Transportation Research Record* 1520 (1996).

### **Contact Information**

**Dr. David Oswald** roswa001@ucr.edu

## Acknowledgments

This research was partially funded by support from the U.S. Department of Energy EcoCAR EV Challenge.

### **Definitions/Abbreviations**

**EV** - Electric Vehicle

**UDDS** - Urban Dynamometer Driving Schedule

**HWFET** - Highway Fuel Economy Driving Schedule

AWD - all-wheel-drive

RWD - rear-wheel-drive

<sup>© 2024</sup> University of California at Riverside. Published by SAE International. No part of this publication may be reproduced, stored in a retrieval system, or transmitted, in any form or by any means, electronic, mechanical, photocopying, recording, or otherwise, without the prior written permission of the copyright holder(s).